Draft version June 12, 2004
Preprint typeset using LaTeX style emulateapj v. 6/6/04

# GALEX OBSERVATIONS OF THE SLOAN DIGITAL SKY SURVEY: A COMPARISON

Mark Seibert[1], Tamás Budavári[5], Jaehyon Rhee[3,1], Soo-Chang Rey[3,1], David Schiminovich[1], Samir Salim[10], D. Christopher Martin[1], Alex. S. Szalay[5], Karl Forster[1], R. Micheal Rich[10], T. Barlow[1], L. Bianchi[2], Y.-I. Byun[3], J. Donas[4], P. G. Friedman[1], T. M. Heckman[5], P. Jelinsky[6], Y.-W. Lee[3], B. F. Madore[7,8], R. Malina[4], B. Milliard[4], P. Morrissey[1], S. Neff[9], O. Siegmund[6], T. Small[1], B. Welsh[6], T. K. Wyder[1]

*Draft version June 12, 2004*

## ABSTRACT

We have matched 358,046 objects in 143 square degrees of overlap between the Galaxy Evolution Explorer (*GALEX*) and the Sloan Digital Sky Survey (SDSS). This paper provides matching statisitics at Medium Imaging Survey and All-sky Imaging Survey depths for SDSS classified stars and galaxies as well as spectroscopic star, galaxy and QSO sub-samples. Distributions of magnitudes, redshifts and colors are provided. Near-ultraviolet (NUV) based color-color diagrams reveal 1) the segregation of main sequence, horizontal branch, sub dwarf, white dwarf, M dwarf, and M dwarf–white dwarf binary stellar populations, 2) a bimodal distribution of galaxies, and 3) the higher signal quality of the *GALEX* NUV compared to the SDSS $u$ band.

*Subject headings:* galaxies: statistics — stars: statistics — surveys — ultraviolet: galaxies — ultraviolet: general — ultraviolet: stars

## 1. INTRODUCTION

As of November 2003, the Galaxy Evolution Explorer (*GALEX*) had observed, in direct imaging mode, ∼143 square degrees of the Sloan Digital Sky Survey's First Data Release (SDSS DR1) footprint (Abazajian et al. 2003). The high quality of the SDSS data, catalogs and object classification provide a context for the interpretation of the *GALEX* ultraviolet (UV) imaging that would be difficult, if not impossible, to achieve otherwise.

We report the results of cross-matching the two data sets in order to provide the astronomical community with an overview of what can be expected from these synergistic surveys. The first public release of *GALEX* data is expected to contain 700–1000 square degrees of overlap. Eventually, *GALEX* will image the entire SDSS survey area, effectively expanding it by two UV bands. Several scientific results have already been derived from this initial limited sample (i.e. Budavari et al. 2004; Salim et al. 2004; Xu et al. 2004; Rich et al. 2004; Bianchi et al. 2004).

In the following sections we describe our method of cross-matching the two surveys, provide basic matching statistics, present UV magnitude distributions, redshift distributions, and explore some examples of the UV/optical color-color space of stars, galaxies, and QSOs.

## 2. OBSERVATIONS

The *GALEX* direct image data include far-UV (FUV; $\lambda_{eff}$=1516 Å, $\Delta\lambda$=256 Å) and near-UV (NUV; $\lambda_{eff}$=2267 Å, $\Delta\lambda$=730 Å) images in circular fields of diameter 1.°2. The spatial resolution is ∼5″. Details of the *GALEX* instrument and data characteristics can be found in Martin et al. (2004) and Morrissey et al. (2004). All magnitudes are in the AB system.

*GALEX* has observed portions of the SDSS footprint at both All-sky Imaging Survey depth (AIS, $t_{\rm exp} \approx 100$ seconds), and Medium Imaging Survey depth (MIS, $t_{\rm exp} \approx 1500$ seconds). 117 AIS and 88 MIS fields overlap 91.92 and 75.08 deg$^2$ of the SDSS respectively. The overlap between any given circular *GALEX* field and the SDSS may be only partial, hence the difference between the sky coverage one might expect for the number of *GALEX* fields and the overlap stated above. Additionally, AIS fields overlap one another and there is some overlap between the AIS and MIS surveys. The former is accounted for in the above, the later is why the 'unique' total overlap is estimated as ∼143 deg$^2$. The overlap is non contiguous.

## 3. CROSS-MATCHING

The method of cross-matching described here was intended to provide the *GALEX* science team with the ability to do early *GALEX*-SDSS investigations. In the near future, public *GALEX* data will be available in relational database form via the Multimission Archive at the Space Telescope Science Institute (MAST[11]). This will allow more sophisticated matching algorithms to be utilized by the entire community.

[1] California Institute of Technology, MC 405-47, 1200 East California Boulevard, Pasadena, CA 91125
[2] Center for Astrophysical Sciences, The Johns Hopkins University, 3400 N. Charles St., Baltimore, MD 21218
[3] Center for Space Astrophysics, Yonsei University, Seoul 120-749, Korea
[4] Laboratoire d'Astrophysique de Marseille, BP 8, Traverse du Siphon, 13376 Marseille Cedex 12, France
[5] Department of Physics and Astronomy, The Johns Hopkins University, Homewood Campus, Baltimore, MD 21218
[6] Space Sciences Laboratory, University of California at Berkeley, 601 Campbell Hall, Berkeley, CA 94720
[7] Observatories of the Carnegie Institution of Washington, 813 Santa Barbara St., Pasadena, CA 91101
[8] NASA/IPAC Extragalactic Database, California Institute of Technology, Mail Code 100-22, 770 S. Wilson Ave., Pasadena, CA 91125
[9] Laboratory for Astronomy and Solar Physics, NASA Goddard Space Flight Center, Greenbelt, MD 20771
[10] Department of Physics and Astronomy, University of California, Los Angeles, CA 90095

[11] http://galex.stsci.edu. MAST is operated by AURA under grant NAG5-7584

Matching is initially performed on a field by field basis. We query the SDSS archive for all primary photometric objects within a 36′ radius of each *GALEX* field center. If an object has associated spectroscopy, that information is also collected. We then cross-match the band-merged *GALEX* catalogs to the SDSS query results. That is, if either an FUV or NUV detection exists we search for a SDSS counterpart. FUV only detections at MIS or AIS depth are rare. Most often these are instrument artifacts but not always. For example, we have found an optical SDSS $z$=3.13 QSO with FUV but no detected NUV flux.

Objects detected by *GALEX* which have no SDSS counterpart typically are either extended, clumpy or diffuse objects which have been decomposed into several smaller objects (shredded) by the standard pipeline[12] processing or are instrument artifacts. Galaxies as small as 10-20″ can be shredded if the light distribution is very irregular. Artifacts are most common near the detector edge ($r$ >30′).

Principal matches are simple nearest neighbors within $r_{\rm m}$=6″. The mean (rms) separation distance for matches in a typical field is 1.″5 (1.″1) – one *GALEX* pixel. 21.6% of *GALEX* detections have multiple SDSS sources within $r_{\rm m}$. The average number of SDSS counterparts within $r_{\rm m}$ for those with multiple detections is 2.1, the average separation of the nearest counterpart is 1.″5, and the average separation of the second nearest is 4.″2. Combining this result with a visual inspection of match quality yields a high degree of confidence for any match with a separation ≤3″. Our catalogs track the distance and position angle of all secondary matches within $r_{\rm m}$ to provide investigators with the ability to apply further restrictions as deemed necessary.

Concatenated match catalogs are then assembled by merging individual field match catalogs. Due to multiple detections of SDSS objects in *GALEX* fields that overlap one another, we take care to establish a one-to-one correlation by using the unique SDSS identifier (objID). For objects detected in multiple fields, we select the one with the highest combined FUV and NUV signal-to-noise (S/N) ratio.

## 4. DISCUSSION

### 4.1. *Match Statistics*

The total densities of *GALEX*–SDSS matches at both MIS and AIS depths are displayed in Table 1. The 'total' category is a good indication of the real object density ($n$) of the *GALEX* MIS ($3.70\times10^3$ deg$^{-2}$) and AIS ($1.01\times10^3$ deg$^{-2}$) surveys. Approximately 14% (4%) of all SDSS objects are detected at MIS (AIS) depth. Matching statistics vary by up to 30% between fields and correlates most strongly with the mean Galactic reddening.

Table 1 further categorizes the matches into photometrically classified stars and galaxies, spectroscopically (sp.) classified stars, galaxies and QSOs, as well as the SDSS 'Main' (flux limited) and 'Red' (color selected) spectroscopic galaxy samples. The percentage of all objects in each category that have NUV or FUV detections with S/N>3 is provided.

The density of stars increases by only a factor of two between the AIS and MIS surveys. In contrast, the density of galaxies increases nearly five fold. With respect to the density of matched spectroscopic objects, there is very little difference between the two types of surveys. Overall, 41% (25%) of galaxies and 11% (5%) of stars have at least 3$\sigma$ detections in the FUV at MIS (AIS) depth.

TABLE 1
*GALEX*-SDSS Match Summary

| Type | MIS $n$[a] (deg$^{-2}$) | MIS S/N>3[b] nuv, fuv (%) | AIS $n$[a] (deg$^{-2}$) | AIS S/N>3[b] nuv, fuv (%) |
|---|---|---|---|---|
| total | 3695.4 | 95, 33 | 1081.3 | 90, 15 |
| stars | 1008.5 | 97, 11 | 536.0 | 96, 5 |
| galaxies | 2686.8 | 94, 41 | 545.3 | 83, 25 |
| sp. stars | 6.4 | 100, 40 | 5.7 | 98, 31 |
| sp. galaxies | 61.3 | 97, 79 | 43.9 | 96, 66 |
| sp. main gal. | 58.7 | 100, 99 | 39.9 | 99, 94 |
| sp. red gal. | 9.5 | 99, 99 | 4.1 | 98, 92 |
| sp. QSO | 12.1 | 99, 72 | 9.7 | 98, 49 |

[a]Detection in either FUV or NUV regardless of error.
[b]Percent of detections with S/N>3 in NUV, FUV.

### 4.2. *Saturation*

Although saturated objects are a tiny fraction of the entire SDSS survey, they can be a non-negligible fraction of *GALEX* surveys. Overall 4.5% (12.4%) of *GALEX* detected objects are saturated in the SDSS at MIS (AIS) survey depth. Only 1.1% (4.5%) of *GALEX* detected SDSS photometrically classified galaxies are saturated at MIS (AIS) depth. Stars, not surprisingly, are far worse. 13.4% of stars at MIS depth are saturated while 20.5% of all stars found at AIS depth are flagged as saturated in the SDSS. Despite the understanding that SDSS saturated objects are stars (regardless of photometric classification) we will exclude them from any plots unless specifically noted.

### 4.3. *Magnitude Distribution*

The distribution of the FUV and NUV magnitudes for the *GALEX*-SDSS matches at MIS depth are displayed in Figure 1. Besides the total distribution (including SDSS saturated objects) we separate into photometrically classified galaxies, stars and saturated objects. In addition, we show the distribution of the spectroscopic galaxy, star, and QSO samples. The distributions are very similar for AIS data, but with lower number densities corresponding to a limiting magnitude 1.5 AB mag brighter.

A detailed analysis of galaxy and star number counts can be found in Xu et al. (2004). We simply note here that galaxies dominate by number for $m_{\rm NUV}\gtrsim$20.5 and $m_{\rm FUV}\gtrsim$18. Saturated objects dominate the bright end of the NUV ($m_{\rm NUV}\lesssim$18.5). In the FUV, saturated objects and stars are equivalent in number at the bright end of the distribution ($m_{\rm FUV}\lesssim$17.5).

### 4.4. *Redshift Distribution*

[12] The source detection and measurement portion of the *GALEX* pipeline is based upon SExtractor (Bertin & Arnouts 1996)

Figure 1 presents the redshift histograms of spectroscopically classified galaxies and QSOs (right top panel). The SDSS 'Main Galaxy' spectroscopic sample is an $r$ band flux limited survey. Although Figure 1 makes it clear that this is not perfectly suited to a UV selected sample, we make no attempt to address completeness issues.

The distribution of galaxies peaks at $z\sim0.1$. 98% of matched galaxies are at $z<0.25$. There is a tail extending out to $z\sim1$. Some of these are misclassified AGN and others are specially targeted luminous red galaxies (LRG) (Abazajian et al. 2003). The redshift distribution of spectroscopic QSOs rises between $0<z<0.2$ and then remains constant out to $z\sim1.9$. The distribution declines between $1.9<z<3.3$. In comparison to the histograms in Figures 2 and 3 of Abazajian et al. (2003), the galaxy histogram here mirrors the DR1 'Main Galaxy' + 'LRG' distribution very well. The DR1 QSO distribution, however, is not flat but continues to rise out to $z\sim1.8$ before turning over.

For galaxies and QSOs with S/N>5 in both the FUV and NUV, the observed UV color as a function of redshift is shown in Figure 1 (right bottom panel). The typical observed UV color of galaxies noticeably reddens from 0.26 when $z<0.025$ to 0.52 for $0.2<z<0.25$. When binned in redhsift intervals of $\Delta z=0.05$, the distribution of UV colors in each interval is Gaussian-like with the notable exception that the lowest redshift bin has a significant tail toward red colors. This red tail decays with increasing $z$, a likely consequence of detecting strongly attenuated and/or old bulge galaxies preferentially at lower redshifts.

The UV color of QSOs varies strongly as a function of redshift. The general trend of turning blue between $0.1< z <0.2$, then turning red between $0.2< z <1.2$, and returning blue-ward for $z >1.2$ is evident in the color versus $z$ panel of Figure 1. The color oscillation is understood as a consequence of Ly$\alpha$ ($\lambda$1216) and C IV ($\lambda$1550) redshifting through the FUV and NUV bands. Beyond $z=1.2$, the Ly$\alpha$ has redshifted beyond the NUV bandpass and the blue colors are the result of the rising extreme-UV blue continuum and Ly$\alpha$ forest.

### 4.5. *Color-Color*

We explore two representative types of color-color diagrams in Figure 2: $m_{\rm NUV}$-$g$ vs. $g$-$r$ and $m_{\rm NUV}$-$u$ vs. $u$-$g$. Each diagram plots combined MIS and AIS data with log scale density contours, where all bands are required to have a S/N$\geq$5. The number of stars ($\sim$60000) and QSOs ($\sim$1300) meeting this requirement is roughly the same for each color. The number of galaxies, however, is very different. There are $\sim$86000 in $m_{\rm NUV}$-$g$ vs. $g$-$r$ and only $\sim$12400 in $m_{\rm NUV}$-$u$ vs. $u$-$g$ due to the much lower signal quality of the SDSS $u$ band. In fact, 83% of galaxies with NUV detections $> 5\sigma$ have $u$ detections $< 3\sigma$.

The middle panel of Figure 2 isolates stars in $m_{\rm NUV}$-$g$, $g$-$r$ space. Late A to K spectral type main sequence (MS) stars form the high density linear feature of $2<m_{\rm NUV}$-$g<8$ and $0<g$-$r<1.1$ (Finlator et al. 2000). Horizontal branch (HB) and A type dwarf stars are a distinct blue population with $g$-$r<0$ and $1< m_{\rm NUV}$-$g<4$ (Yanny et al. 2000). The extreme blue tail of both colors ($m_{\rm NUV}$-$g<1$ and $g$-$r<0.2$) consists of degenerate white dwarfs (Lenz et al. 1998) and high surface gravity sub-dwarf O and B stars (sdO/sdB).

There is also a population of stars at low density which saturate at $g$-$r\sim1.4$, yet have a broad range of $m_{\rm NUV}$-$g$ colors. The optical colors suggest they are M dwarfs (Finlator et al. 2000). It is very likely that we are also probing the M dwarf–white dwarf bridge recently discovered by Smolčić et al. (2004). The faint 'bridge' of stars extending from the main M-dwarf population at $g$-$r\sim1.4$ toward the white dwarf population are M dwarf–white dwarf binary systems whose color depends upon the luminosity ratio. Smolčić et al. (2004) find 0.4 deg$^{-2}$ in the entire DR1 (2099 deg$^2$) using colors involving all 5 SDSS bands. Repeating their selection technique with the higher signal quality of *GALEX* NUV relative to $u$, we find the density of these objects to be at least a factor of two higher.

The remaining objects are those at the common locus of QSOs and blue galaxies, and suffer strong contamination by them. Only 8% of the stars in this plot have FUV detections of at least $3\sigma$ and they are concentrated in the white dwarf/sdO/sdB, HB and QSO contamination regions.

The right panel of Figure 2 isolates galaxies in $m_{\rm NUV}$-$u$, $u$-$g$ space. Although weak, there is a clear bimodality present. The same is true in $m_{\rm NUV}$-$g$, $g$-$r$ space with 7 times as many galaxies. Bimodality in both color and spectroscopic parameters has been a topic of considerable recent interest (Baldry et al. 2004; Kauffmann et al. 2003; Strateva et al. 2001) and it was not clear that it would be present in a UV selected sample. Inspection of the color magnitude diagrams for the sample confirms that $m_{\rm NUV}$-$u$=2.2 delineates the two populations here. The blue ($m_{\rm NUV}$-$u$ <2.2) galaxies strongly dominant by number (92%) relative to the red ($m_{\rm NUV}$-$u$ >2.2) galaxies.

We have computed the spectrophotometric colors of the galaxies from the Storchi-Bergmann et al. database of UV-optical spectra and over-plot them on the $m_{\rm NUV}$-$u$ vs. $u$-$g$ diagram. Starburst galaxies reside principally in the bluest regions. Ellipticals tend to lie within the red galaxy space. Spirals, Seyferts and Liners span the color space between them. 88% (36%) of blue (red) galaxies have FUV detections of at least $3\sigma$. Given that the sample is essentially NUV selected, the high fraction of red galaxies (presumably early-type galaxies) with FUV emission is understandable.

## 5. SUMMARY

We have described the method and initial results of matching 143 deg$^2$ of *GALEX* survey fields with the SDSS. At MIS survey depth, there are $3.7\times10^3$ objects per square degree (14% of the SDSS density) of which $\sim$33% are also detected in the FUV.

SDSS saturated objects can be a non-negligible fraction of matches at AIS survey depth where 20% of stars are flagged as saturated. Saturated SDSS objects dominate the bright end of the matched surveys but only represent 4.5% of all objects at MIS depth.

The spectroscopic galaxy sample redshift distribution peaks near $z=0.1$ with 98% at $z <0.25$. Noticeable reddening of the mean UV color occurs over this redshift range [$\Delta$(FUV-NUV)=0.26]. QSOs are detected out to a $z$ of 3.3 and the UV color oscillates strongly over this range due to the redshifting of Ly$\alpha$ and C IV.

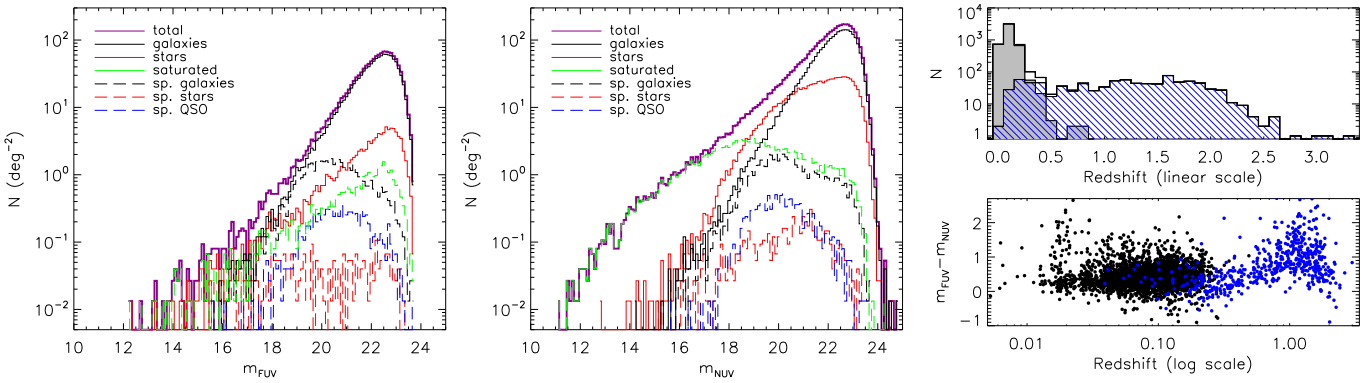


FIG. 1.— The FUV (LEFT) and NUV (MIDDLE) magnitude distributions of MIS *GALEX*-SDSS matches. Magnitudes are corrected for foreground extinction. RIGHT-TOP: The redshift distribution of spectroscopically classified galaxies and QSOs in MIS data. The thick black line is the total distribution. The gray histogram represents galaxies while the hashed region is the distribution of QSOs. RIGHT-BOT: UV color versus redhsift of high signal-to-noise galaxies (black) and QSOs (blue).

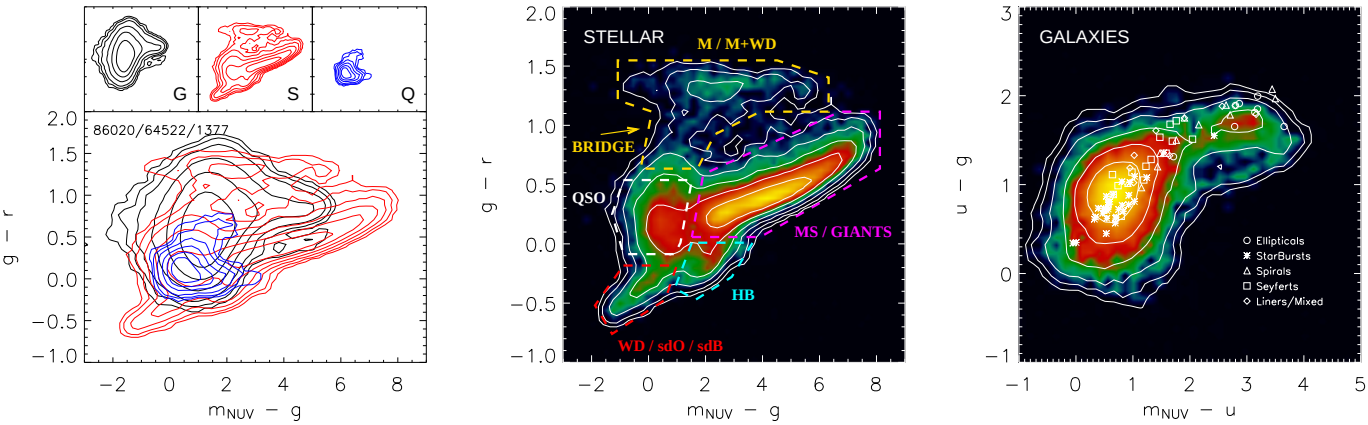


FIG. 2.— Log scale number density color-color plots. LEFT: $m_{NUV}$-g vs. g-r. The small panels separate photometrically classified galaxies (black, G), stars (red, S) and spectroscopic QSOs (blue, Q). Contours are 5, 10, 20, 40, 60, and 80% of maximum. The large panel superimposes the contours for all types. The total number of each class of object appears in the upper left in the order galaxies/stars/QSOs. MIDDLE: $m_{NUV}$-g vs. g-r for only stars. Polygons highlight regions for several stellar populations (see text). RIGHT: $m_{NUV}$-u vs. u-g for only galaxies. Overlayed are the spectrophotometric colors of a variety of galaxy types (see text).

Inspection of NUV based color-color diagrams reveals the segregation of MS, HB, white dwarf, sub-dwarf, M dwarf and M dwarf–white dwarf binary stellar populations. Galaxies exhibit a weak bimodality in NUV based color-color plots between blue star forming galaxies (starbursts, spirals) which have a high incidence of FUV emission and red galaxies (ellipticals) which have a low incidence of FUV emission. $m_{NUV}$-$u$=2.2 delineates the two populations.

We show the significant quality difference between the SDSS $u$ band and the *GALEX* NUV by noting that 83% of galaxies with S/N> 5 in the NUV have S/N< 3 in $u$. The number density of M dwarf–white dwarf binaries found with the *GALEX* NUV is at least twice as high as that found with $u$. For applications which do not require the full image resolution of the SDSS, the *GALEX* NUV band may be a superior alternative.

We gratefully acknowledge NASA's support for construction, operation, and science analysis for the *GALEX* mission, developed in cooperation with the Centre National d'Etudes Spatiales of France and the Korean Ministry of Science and Technology.

REFERENCES

Abazajian, K., et al. 2003, AJ, 126, 2081
Baldry, I. K., et al. 2004, ApJ, 600, 681
Bertin, E. & Arnouts, S. 1996, A&AS, 117, 393
Bianchi, L., et al., 2004. ApJ, present volume.
Budavari, T., et al., 2004. ApJ, present volume.
Finlator, K., et al. 2000, AJ, 120, 2615
Kauffmann, G., et al. 2003, MNRAS, 341, 33
Lenz, D. D., et al. 1998, ApJS, 119, 121
Martin, D. C. , et al. 2004. ApJ, present volume.
Morrissey, P., et al. 2004. ApJ, present volume.
Rich, M., et al., 2004. ApJ, present volume.
Salim, S., et al., 2004. ApJ, present volume.
Smolčić, V., et al. 2004, astro-ph/0403218
Strateva, I., et al. 2001, AJ, 122, 1861
Yanny, B., et al. 2000, ApJ, 540, 825
Xu, K., et al., 2004. ApJ, present volume.